Available online at www.sciencedirect.com
ScienceDirect
European Journal of Medicinal Chemistry 44 (2009) 558–567
EUROPEAN JOURNAL OF MEDICINAL CHEMISTRY
http://www.elsevier.com/locate/ejmech

Original article

Discovery of a new family of bis-8-hydroxyquinoline substituted benzylamines with pro-apoptotic activity in cancer cells: Synthesis, structure–activity relationship, and action mechanism studies

Vincent Moret [a], Younes Laras [a], Thierry Cresteil [b], Geneviève Aubert [b], Dou Q. Ping [c], Chen Di [c], Magali Barthélémy-Requin [d], Christophe Béclin [d], Vincent Peyrot [e], Diane Allegro [e], Amandine Rolland [a], Francesca De Angelis [g], Evelina Gatti [g], Philippe Pierre [g], Luca Pasquini [f], Eleonora Petrucci [f], Ugo Testa [f], Jean-Louis Kraus [a,*]

[a] *Laboratoire de Chimie Biomoléculaire, IBDML-UMR-6216-CNRS, Faculté des Sciences Luminy, Université de la Méditerranée, Parc Scientifique de Luminy, Case 901, 13288 Marseille Cedex 9, France*
[b] *Institut de Chimie des Substances Naturelles, CNRS UPR 2301, Avenue de la Terrasse, 91198 Gif sur Yvette, France*
[c] *The Prevention Program, Barbara Ann Karmanos Cancer Institute, Department of Pathology, School of Medicine, Wayne State University, 540.1 HWCRC, 4100 John R. Road, Detroit, MI 48201-2013, USA*
[d] *IMVT-IBDML, Campus de Luminy, Case 907, 13288 Marseille Cedex 09, France*
[e] *FRE CNRS 2737, Faculté de Pharmacie, 27 Boulevard Jean Moulin, 13385 Marseille Cedex 5, France*
[f] *Department of Hematology, Oncology and Molecular Medicine, Instituto Superiore di Sanità, 00161 Rome, Italy*
[g] *Centre d'immunologie Marseille-Luminy, CNRS-UMR-6102-INSERM 631, Case 906, 13288-Marseille Cedex 9, France*

Received 7 January 2008; received in revised form 21 March 2008; accepted 27 March 2008
Available online 10 April 2008

Abstract

Bis-8-hydroxyquinoline substituted benzylamines have been synthesized and screened for their antitumor activity on KB3 cell line model. Synthesis of this series of new analogues was accomplished using a one pot specific methodology which allows the synthesis of both bis- and mono-8-hydroxyquinoline substituted benzylamines. Among the synthesized compounds two compounds (**4a** and **5a**), respectively, named *JLK 1472* and *JLK 1486*, were particularly potent on KB3 cell line. Their CC_{50} values being, respectively, 2.6 and 1.3 nM. Screened on a panel of cell lines showing various phenotype alterations, both compounds were found inactive on some cell lines such as PC3 (prostate cell line) and SF268 (neuroblastoma cell line) while highly active on other different cell lines. Mechanistic studies reveal that these two analogues did not affect tubulin and microtubules neither they exert a proteasomal inhibition effect. In contrast **4a** and **5a** activate specifically caspase 3/7 and not caspase 8 and 9, suggesting that their biological target should be located upstream from caspase 3/7. Moreover their cytotoxic effect is potentiated by the pro-apoptotic effects of TRAIL.

Keywords: Bis-hydroxyquinoline; Benzylamine; Cytotoxic; Synthesis; KB3 cell line; Apoptosis

1. Introduction

There are generally two different approaches used for anti-proliferative activity compound hit identification. The reverse chemical biology approach, or target-based approach, consists first in the identification of a compound that activates or inhibits a specific target and then in the search for a phenotype induced by the compound in vivo. The forward chemical biology approach, or phenotype-based approach, starts with an outward physical characteristic or phenotype and ends with the identification of the responsible target; in this case, molecules are screened for ''hits'' that induce a particular phenotype before

* Corresponding author. Tel.: +33 491 82 91 41; fax: +33 491 82 94 16.
E-mail address: kraus@luminy.univ-mrs.fr (J.-L. Kraus).

0223-5234/$ - see front matter © 2008 Elsevier Masson SAS. All rights reserved.
doi:10.1016/j.ejmech.2008.03.042

the cellular target is identified. Both reverse and forward approaches have yielded clinically useful agents for cancer management.

The approach we have used for the discovery of new active anticancer drugs is the forward chemical biology approach. Our house chemical library of bioactive molecules was first screened on KB3-1 (human mouth epidermal carcinoma) cell lines as primary screening in order to identify analogues which present cytotoxic activity on this cell line model [1]. From this, we have identified a new series of small molecules, incorporating in their structure a hydroxyquinoline moiety, which presented potent cytotoxic effect on KB3-1 cells. Indeed, this cell line appears to be a representative and suitable model, since it is known to be very sensitive to drugs and also because a P-gp induced cell line, is also available [2].

Starting from these preliminary results, in this paper we report the synthesis of a series of compounds based on this hydroxyquinoline scaffold, and their in vitro nanomolar range cytotoxic activity on KB3 and other cell lines from different histogenetic origin having various phenotype alterations. We also report the ability of this new family of compounds to induce caspase activation since it is known that caspases play an important role in apoptosis induced by genotoxic stress, and that some anticancer drugs trigger mitochondrial outer membrane permeabilization resulting in cytochrome *c* release and caspase activation [3,4]. We have also investigated the possible activity for these new analogues to act as proteasome inhibitors as well as promotor of α, β tubulin assembly.

2. Chemistry

Among the tested compounds from our in house library, analogues whose general structure included an 8-hydroxyquinoline moiety linked to a substituted benzylamine (Fig. 1) were found cytotoxic for KB3-1 cells at concentrations ranging around 1 μM.

In order to optimize the cytotoxic effect found for some members of this family of compounds, we synthesized several new analogues based on this scaffold, in which specific substituents R_1 and R_2 were introduced.

The synthetic scheme which has been developed in order to elaborate this library is outlined in Scheme 1.

Starting from 8-hydroxyquinoline (**1**), the required starting material 5-chloromethyl 8-hydroxyquinoline (**2**) was obtained in good yield, using a known procedure [5]. The news analogues have been synthesized, using standard methodologies,

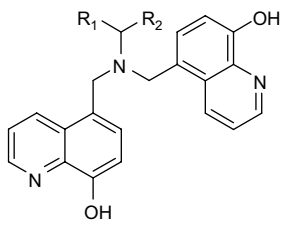

Fig. 1. General structure of the new cytotoxic drugs.

which involved the direct condensation of 5-chloromethyl 8-hydroxyquinoline (**2**) and various substituted primary benzylamines. This reaction was performed in the presence of potassium carbonate in acetonitrile and gives a mixture of mono- and bis-hydroxyquinoline derivatives. The bis-quinoline compounds (**3a–9a**) are first isolated from the mixture using their insolubility in diethyl ether. The mono substituted compounds are isolated from the remaining mixture using the Boc protection procedure. The Boc protected analogues (**5c**, **7c** and **8c**) is isolated by column chromatography and then deprotected to give the corresponding mono-hydroxyquinoline analogues (**3b–5b**, **7b–8b**). The whole compounds including the Boc analogues were fully characterized and submitted to KB3-1 cell line model screening.

For mechanistic and structure–activity relationship purposes, we have also synthesized a representative quinoline analogue (**14**), which structure differs from the most potent analogue by the absence of the hydroxyl group at the 8-position of the heterocyclic ring. Its synthesis is depicted in Scheme 2.

Starting from the quinoline-5-carboxylic acid (**10**) which was first transformed into its corresponding ethyl ester (**11**) and reduced with lithium aluminium hydride, the corresponding alcohol **12** was obtained according to a known procedure [6]. Chloration of **12** in the presence of thionyl chloride lead to the corresponding chloromethylquinoline **13** (67% yield). Condensation of **13** with 4-trifluoromethylbenzylamine in the presence of potassium carbonate lead to the expected bis-quinoline **14**.

3. Results and discussion

3.1. Primary screening: cytotoxic activity on KB3-1 cell line

All compounds were evaluated for their cytotoxic effect on KB3 cell line according to a procedure described in Section 5. The obtained results are presented in Tables 1 and 2.

From the CC_{50} values presented in Tables 1 and 2, it appears that derivatives belonging to the bis-hydroxyquinoline series (**3a–9a**) are more active than the mono-hydroxyquinoline analogues. The CC_{50} values of the former ranged from 1.3 to 123 nM whereas the cytotoxic activity values of the corresponding mono-hydroxyquinoline derivatives (**3b–5b**, **7b–9b**) were found far less active, since their cytotoxic activity values lie between 1 and 10 μM.

The importance of the substituents (R_1) at various positions of the benzyl moiety was first examined (Table 1). Introduction of a trifluoromethyl substituent at the 4-position of the aromatic ring led to the most potent analogue (**5a**, $CC_{50} = 1.3$ nM). Varying the inductive electronic effect (electron-withdrawing substituent NO_2 (**6a**) and electron-donating substituent CH_3 (**4a**)) did not change drastically the potency of the resulting analogues. Their CC_{50} values varied only by one order magnitude, from 1.3 to 42 nM, indicating that the compounds are still potent cytotoxic drugs. It could also be observed that the *para* position, on which CF_3 group was introduced on the benzyl group, appears to be the most

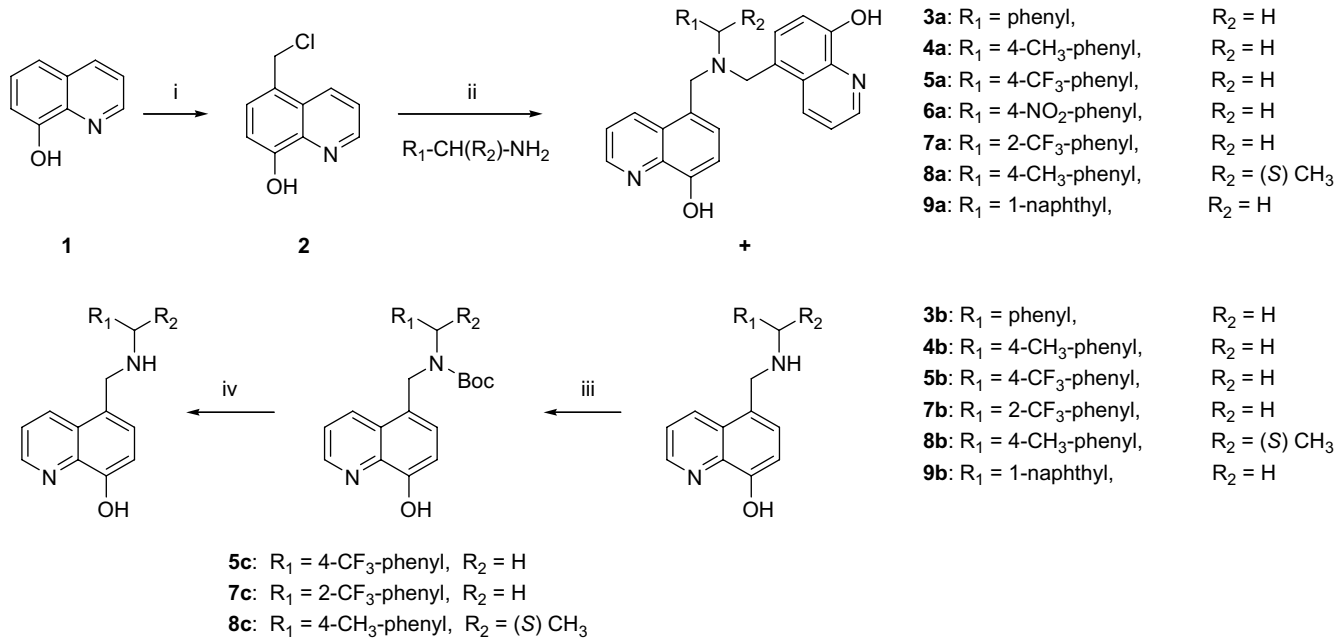

Scheme 1. Reagents and conditions: (i) HCHO, 37% HCl in H_2O, HCl (gas), rt, overnight, 80%; (ii) $CHCl_3$, rt, 24 h; or K_2CO_3, CH_3CN, rt, 24 h; (iii) $(^tBoc)_2O$, EtOAc; (iv) HCl, Et_2O, rt, 4 h.

favourable position for optimum cytotoxic activity. Indeed compound **5a** in which CF_3 is located at the *para* position being two logs more active than its corresponding analogue in which CF_3 group is introduced at the *ortho* position (**7a**). Moreover, introduction of a methyl group on the methylene of the benzyl group (**8a**, $CC_{50} = 41$ nM) only slightly diminished the resulting cytotoxic activity compared to its corresponding analogue (**4a**, $CC_{50} = 2.6$ nM). Encouraged by these results, we next prepared the corresponding analogue of the most potent compound **5a** in which both hydroxy substituents were removed on the quinoline heterocycles leading to compound **14**. We found that this latter analogue was two logs less active than its corresponding compound **5a**, indicating that the presence of the hydroxyquinoline moiety was required for cytotoxic activity.

The whole obtained results from this primary screening led us to select compounds **4a** and **5a**, which are, respectively, named *JLK 1472* and *JLK 1486*, as representative hits which could be submitted to further mechanistic investigations.

3.2. Activity of the new drugs on various cancer cell lines

The cytotoxic activity of compounds *JLK 1472* and *JLK 1486* was further investigated on a panel of human cancer cell lines and on two non-cancerous cell lines (Table 3).

From these results several observations can be made.

- The prostate cell line PC-3 required higher CC_{50} for both drugs than other cell lines.
- SF268 (neuroblastoma cell line) is also poorly affected by both drugs.
- OV3 are ovarian tumor cell lines.
- A549 are human alveolar epithelial cell lines.
- HepG2 are human hepatocellular liver carcinoma cell lines.
- MCF7R and HCT15 are derived from MCF7 (epithelial breast cancer cell line) and HCT116 cell lines (colonic epithelial cell line), respectively, after chemical exposure. It has been shown that these two cell lines expressed the

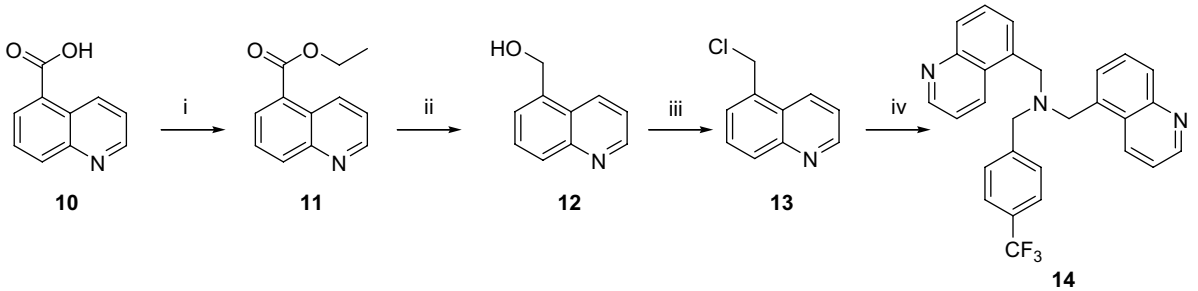

Scheme 2. Reagents and conditions: (i) HCl gas, Et_2O, reflux, 20 h; (ii) $LiAlH_4$, Et_2O, 0 °C, 1.5 h; (iii) $SOCl_2$, reflux, 2 h, 67%; (iv) 4-trifluoromethylbenzylamine, K_2CO_3, DMF, 70 °C, 4 h, 65%.

Table 1
Cytotoxic effect on KB3-1 cell lines of bis-hydroxyquinoline compounds

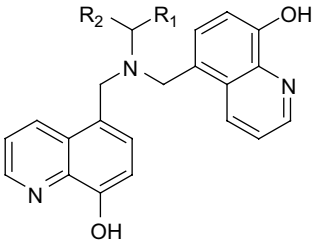

Compound	R_1	R_2	CC_{50} (nM)
3a	Phenyl	H	15
4a (*JLK 1472*)	4-CH_3–phenyl	H	2.6
5a (*JLK 1486*)	4-CF_3–phenyl	H	1.3
6a	4-NO_2–phenyl	H	42
7a	2-CF_3–phenyl	H	123
8a	4-CH_3–phenyl	(*S*)CH_3	41
9a	1-Naphthyl	H	5
Docetaxel			0.25

P-gp protein. The level of expression of P-gp, much higher in MCF7R than in HCT15 cells, could be associated with the shift of CC_{50} values displayed compared to the native MCF7 and HCT116 cells. However, the variation in the CC_{50} is relatively moderate and would suggest that analogues *JLK 1472* and *JLK 1486* could be possible P-gp substrates but with a low affinity.

- Leukaemia cells (HL60 and K562) are also sensitive to both drugs.

3.3. Action mechanism studies

3.3.1. Tubulin and microtubule studies

As far as the observed effects of paclitaxel or Taxol® on our model of KB3 cells were found very potent ($CC_{50} = 0.1$ nM),

Table 2
Cytotoxic effect on KB3-1 cell lines of mono-hydroxyquinoline compounds

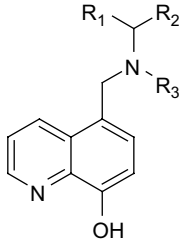

Compound	R_1	R_2	R_3	CC_{50} (μM)
3b	Phenyl	H	H	>1
4b	4-CH_3–phenyl	H	H	>10
5b	4-CF_3–phenyl	H	H	10
7b	3-CF_3–phenyl	H	H	0.2
8b	4-CH_3–phenyl	(*S*)CH_3	H	>1
9b	1-Naphtyl	H	H	>1
5c	4-CF_3–phenyl	H	^{t}Boc	10
7c	3-CF_3–phenyl	H	^{t}Boc	1
8c	4-CH_3–phenyl	(*S*)CH_3	^{t}Boc	>1
Docetaxel				0.25

Table 3
In vitro cell growth inhibition by analogues *JLK 1472* and *JLK 1486* in a panel of cell lines of different histogenic origin and having various phenotype alterations

Cell lines	Compounds CC_{50} (nM)	
	JLK 1486	*JLK 1472*
KB3	1.5 ± 0.1	8.5 ± 2.9
HCT116	1.0 ± 0.1	3.2 ± 1.2.
HCT15	0.8 ± 1.0	6.0 ± 7.3
MCF7	1.2 ± 0.3	5.4 ± 0.9
MCF7R	4.7 ± 1.3	37.3 ± 28
OV3	3.0 ± 0.1	8.0 ± 0.4
PC3	206 ± 113	343 ± 125
A549	0.9 ± 0.2	4.3 ± 0.1
SF268	91 ± 49	178 ± 83
HL60	10.9 ± 4.9	32.7 ± 6.6
K562	5.2 ± 8.2	40.8 ± 22
HepG2	22.8 ± 39.2	52.1 ± 14.5

we investigate if compound *JLK 1486* could act as Taxol®-like drug. Indeed, suppression of the cellular microtubule dynamics by Taxol® is the main cause of cell division inhibition and of tumor cell death [7].

In this perspective, we evaluated the ability of *JLK 1486* to modify the in vitro assembly of tubulin by a standard turbidimetric method. The tubulin self-assembly into microtubules in the presence of *JLK 1486* is shown (Fig. 2). In our conditions, when 20 μM of tubulin with 20 μM of *JLK 1486* compound (curve B, dashed line) and without (curve A, solid line) are incubated at 37 °C the turbidity time courses are similar, demonstrating that *JLK 1486* did not inhibit microtubule formation.

Moreover, when the sample in the presence of *JLK 1486* compound is cooled down to 4 °C, there is a complete disassembly, indicating a lack of tubulin dimer aggregation or microtubule stabilization by the ligand. Taxol® is known to promote tubulin dimer assembly by binding to β-tubulin in microtubules. We checked if *JLK 1486* induced microtubule formation at a tubulin concentration which did not permit microtubule formation. Curve B showed that *JLK 1486* (dashed line) was unable to induce microtubule formation.

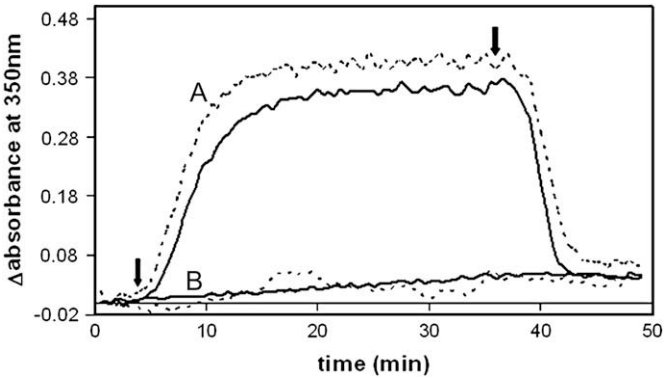

Fig. 2. Effects of *JLK 1486* on the turbidity time course of in vitro microtubule assembly. The tubulin assembly curve is given as a solid line, whereas tubulin assembly with *JLK 1486* (ratio tubulin: *JLK 1486* 1:1) is given as a dashed line. Tubulin concentration was 20 μM for A and 15 μM for B. Assembly is started by heating the solution from 4 to 37 °C (first arrow) and the disassembly is induced by switching the temperature to 4 °C (second arrow).

No direct inhibitory concentration effect of the drug on the tubulin assembly was observed, neither a stabilizing effect on microtubule formation. These results suggest that the new discovered drugs are not inhibitors of microtubule formation Taxol-like drugs [8].

3.3.2. Proteasomal activity

We next examined whether the most active analogues could affect the proteasome activity. It has been reported that hydroxyquinolines are compounds capable of forming stable complexes with cooper(II) ions [9]. Similarly, clioquinol, a known copper chelatant, which structure included an 8-hydroxyquinoline moiety (Fig. 3) used as an antibiotic for treating diarrhea and skin infection [10], has been identified as an androgen receptor inhibitor and an inducer of cellular apoptosis in relation with its observed antiprostate tumor effect [11]. Clioquinol, after binding to copper, can inhibit the proteasomal chymotrypsin-like activity and can induce cell death in human cancer LNCaP and C4-2B cell lines [11].

So it can be hypothesized that *JLK 1486* (**5a**) and *JLK 1472* (**4a**) could exert their antiproliferative activities through an inhibition of the cellular proteasome in a copper-dependent manner. To test this possible mode of action we assessed the antiproliferative activity of compounds *JLK 1486* and *JLK 1472* on the HL60 cell line and compare their effect with that of clioquinol used as a model.

As shown in Fig. 4A, clioquinol alone had no antiproliferative activity in HL60 cells when incubated for 24 h in the absence of $CuCl_2$, but elicited a dramatic reduction of cell proliferation and viability (as shown by the trypan blue exclusion assay) in the presence of $CuCl_2$ (Fig. 4A). This clearly suggests that *JLK 1472* and *JLK 1486*, unlike clioquinol, acted through an independent mechanism. Concomitantly, it was capable to promote the cleavage of PARP in the presence of $CuCl_2$ whereas *JLK 1486* had no or very limited effect on the processing of PARP (Fig. 4B). Since PARP is a caspase 3 substrate, it did not represent a direct proteasome marker, we have performed a direct in vitro proteasome inhibitory test using both chymotrypsin and trypsin sensitive peptides in the presence of various concentrations of *JLK 1486* from 1 to 1 μM. No activity proteasomal inhibitory activity was found (Fig. 5), establishing definitively the lack of effect of *JLK 1486* on proteasomal activity.

3.3.3. Caspase activation

We next investigated whether the cytotoxic activity of *JLK 1472* and *JLK 1486* on HL60 cell line depends on caspase induction.

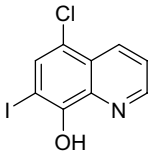

Fig. 3. Clioquinol.

For this purpose we explored their capacity to activate caspase by a direct measurement of caspase activities in HL60 cells after a 48 h exposure to these compounds [4]. To assess the role of *JLK 1472* and *JLK 1486* on the caspase cascade we used specific substrates: DEVD for caspases 3/7, IEDT for caspase 8 and LEHD for caspase 9. Colchicine was used as a positive reference inducer, and compounds *JLK 1472* and *JLK 1486* were tested at three concentrations 1, 0.1 and 0.01 μM. *JLK 1472* and *JLK 1486* had no effect upon caspase 3/7 activation at the concentration of 0.01 μM, but elicited a marked effect at 0.1 and 1 μM (Fig. 6). Assayed in parallel in the same samples, caspase 8 and caspase 9 were not activated by both compounds even at 1 μM. Thus *JLK 1472* and *JLK 1486* activated caspases 3/7 in a dose-dependent manner but did not induce caspase 8 nor 9 activation.

3.3.4. Drug cytotoxic effect potentiation by TRAIL (tumor necrosis factor related apoptosis inducing ligand) [12]

Since it was shown above that *JLK 1486* and *JLK 1472* induce caspase 3/7 activation, we evaluated whether their cytotoxic effect is potentiated by the death ligand TRAIL. In this purpose, we have used four cancer cell lines, either scarcely (M4, A2780/WT and A2780/ADR) or moderately (HL60 and MCF7) sensitive to the pro-apoptotic effects of TRAIL.

As shown in Fig. 7 it can be seen that the simultaneous addition of *JLK 1486* and TRAIL, even using *JLK 1486* at low concentrations (10 nM for HL60 cells or 100 nM for A2780, M4 and MCF7cells) that were only moderately cytotoxic, resulted in a strong apoptotic effect with a high rate of cell death (Fig. 7).

4. Conclusion

From in vitro cellular screening on KB3 cell line, we have discovered a new family of potent cytotoxic drugs, which belong to the class of bis-8-hydroxyquinoline substituted benzylamine, which have never been described before. From the elaboration of a small focussed library, two analogues of this family were found particularly potent on KB3 cell lines (analogue *JLK 1472* and *JLK 1486*); their cytotoxic activity (CC_{50} ranging from 1 to 5 nM) was only one order magnitude less potent than that of the standard clinically used anticancer drug, docetaxel.

Experiments on HL60 cell line using different substrates have shown that these compounds can activate caspase 3/7 between 1 and 0.1 μM but not at 0.01 μM. These range of concentrations correspond to the concentrations that are able to induce cytotoxicity in the same cell line, suggesting that cell death induced by these compounds occurs through a caspase 3/7 apoptosis pathway. This assumption is further supported by the observation that cytotoxicity in HL60 is further enhanced in the presence of TRAIL which is also able to induce caspase 3/7. Since different pathways may induce apoptosis in cell, we have investigated the possible involvement of two pathways known to be targeted by different clinical anticancer drugs, microtubule assembly and proteasome. However none of these pathways appeared to be affected by *JLK 1472* and *JLK 1486*, showing that these two compounds act through different pro-apoptotic pathways.

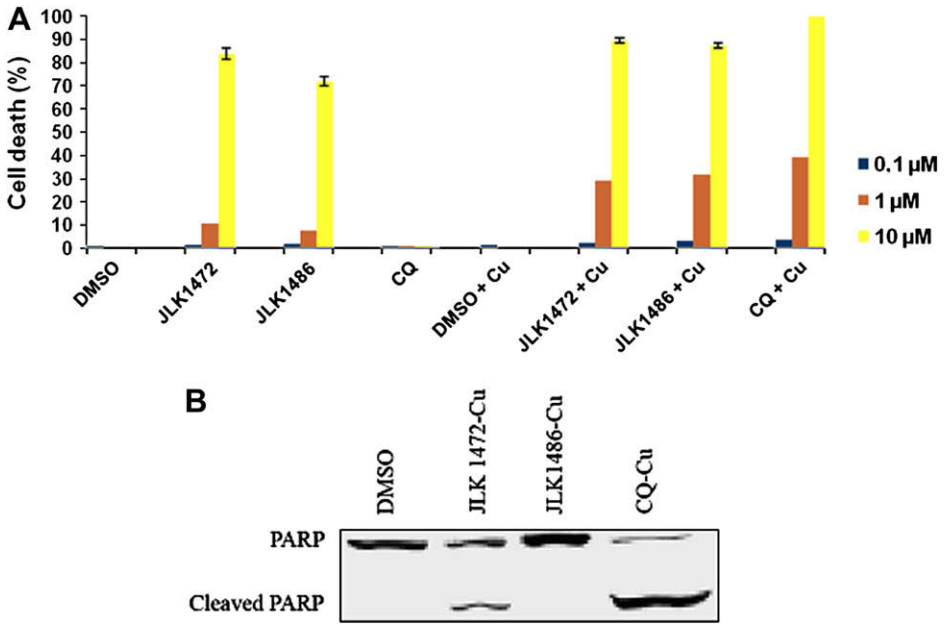

Fig. 4. Comparative cytotoxicity of clioquinol, *JLK 1472* and *JLK 1486* in the absence or presence of copper (A) and Western blotting (B). The reduction of cell viability by *JLK 1472* and *JLK 1486* on human leukaemia HL60 cells was compared with that of clioquinol (CQ). HL60 cells were treated for 24 h with *JLK 1472*, *JLK 1486* or CQ (A), or treated with a mixture of *JLK 1472*, *JLK 1486* or CQ with $CuCl_2$ in the indicated concentrations (A), followed by trypan blue assay (A) or Western blotting (B) at 10 µM drug concentration.

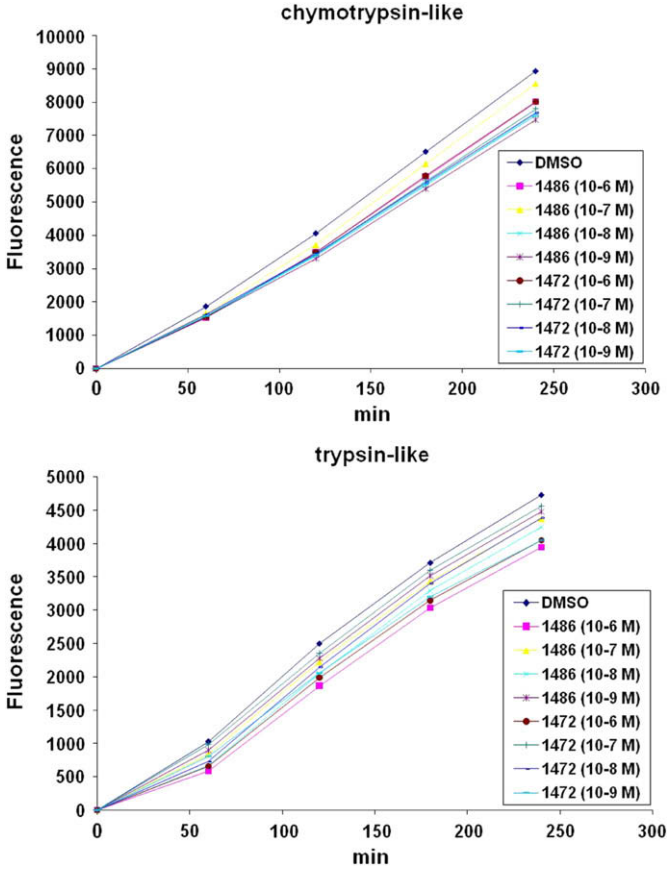

Fig. 5. Proteasomal activity of analogues *JLK 1472* and *JLK 1486*.

Further investigations are needed in order to identify the biological target on which these new drugs are acting. Moreover pharmacokinetic studies should be performed in order to evaluate a possible therapeutical interest for these new drugs.

5. Materials and methods

5.1. Chemistry

5.1.1. General procedures

Unless otherwise noted, starting materials and reagents were obtained from commercial suppliers and were used without purification. Methylene dichloride (CH_2Cl_2) was distilled over P_2O_5 just prior to use. Acetonitrile was of anhydrous quality from commercial suppliers (Aldrich, Carlo Erba Reagents). As far as the products are obtained as a mixture of multiple compounds (2 or 3), the given yields are the calculated yields for each compound and not the overall yield of the reaction. ^1H NMR spectra were recorded at 250 MHz on a Bruker AC-250 spectrometer. Chemical shifts are expressed as δ units (parts per million) downfield from TMS (tetramethylsilane). Electro-spray mass spectra were obtained on a Waters Micromass ZMD spectrometer by direct injection of the sample solubilized in acetonitrile. Elemental analyses were within ±0.4% of theoretical values for all compounds. All reactions were monitored by thin-layer chromatography. Analytical thin-layer chromatographies (TLC) were performed using silica gel plates of 0.2 mm thick ($60F_{254}$ Merck). Preparative flash column chromatographies were carried out on silica gel (230–400 mesh, G60 Merck).

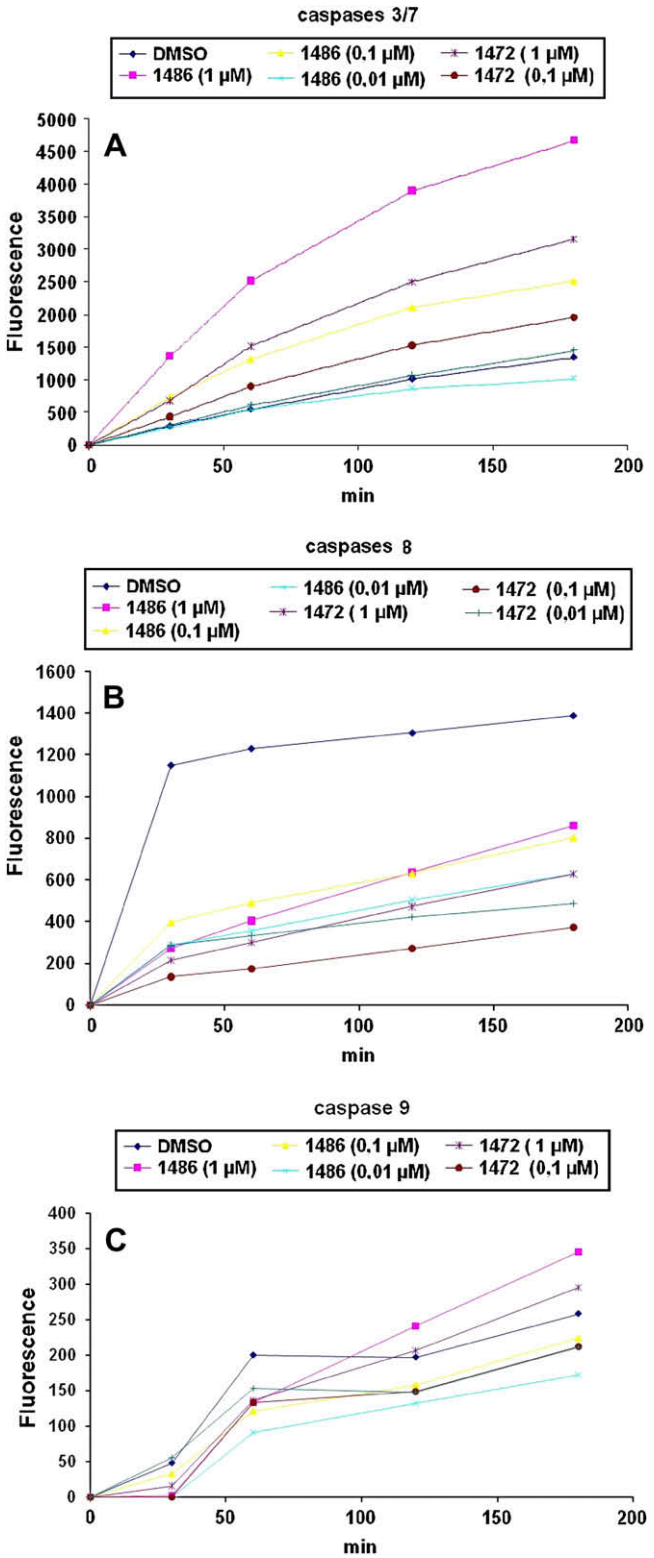

Fig. 6. Caspase activation by analogues *JLK 1472* and *JLK 1486*.

*5.1.2. 5,5′-(Benzylazanediyl)bis(methylene)diquinolin-8-ol (**3a**) and 5-((benzylamino)methyl)quinolin-8-ol dihydrochloride (**3b**)*

A solution of 5-chloromethylquinolin-8-ol dihydrochloride (300 mg, 1.3 mmol) and benzylamine (419 mg, 3.91 mmol) in ethyl acetate (10 ml) is stirred at 50 °C overnight. It is cooled to 0 °C and filtered; the filter cake is washed with cold ethyl acetate (5 ml). The filtrate is concentrated in vacuo, diluted in diethyl ether (5 ml) and centrifuged. The etheral phase is removed and the obtained solid is washed two more times by centrifugation with diethyl ether at 0 °C to give 168 mg of **3a** (30% yield) as a green powder; ^{1}H NMR ($CDCl_3$) δ 3.66 (s, 2H), 3.99 (s, 4H), 7.20–7.35 (m, 6H), 7.42–7.45 (m, 3H), 7.55–7.58 (m, 2H), 8.03–8.07 (m, 2H), 8.89 (s, 2H); ^{13}C NMR ($CDCl_3$) δ 56.4, 58.5, 108.8, 120.8, 125.2, 127.2, 127.6, 128.1, 129.7, 129.8, 134.3, 138.6, 139.0, 147.5, 151.8; ESI-MS $m/z = 422$ ($[M + H]^+$, 100%). Combined ethereal phases are concentrated in vacuo. The obtained product is dissolved in dichloromethane (4 ml) and Boc_2O (171 mg, 0.786 mmol) is added. The solution is stirred overnight at room temperature then washed with water (4 ml) and brine (2 ml). It is dried over $MgSO_4$ then concentrated in vacuo and purified by chromatography eluting with cyclohexane–dichloromethane (1:1). The obtained product is dissolved in diethyl ether (2 ml) and hydrochloric acid in diethyl ether (1 M, 2 ml) is added. The solution is centrifuged to give 70 mg **3b** as a white solid (21% yield); ^{1}H NMR (MeOH-d_4) δ 4.2 (s, 2H), 4.6 (s, 2H), 7.2–8.0 (m, 8H), 8.9 (s, 2H); ^{13}C NMR (MeOH-d_4) δ 41.2, 43.6, 49.1, 113.9, 116.7, 120.8, 127.4, 128.1, 130.6, 132.7, 140.9, 141.1, 146; ESI-MS $m/z = 265$ (free base, $[M + H]^+$, 100%).

*5.1.3. 5,5′-(4-Methylbenzylazanediyl)bis(methylene) diquinolin-8-ol (JLK 1472, **4a**) and 5-((4-methylbenzylamino)methyl)quinolin-8-ol dihydrochloride (**4b**)*

The compounds were synthesized from 4-methylbenzylamine following the procedure described for **3a** and **3b**. Compound **4a**: yield 22%; ^{1}H NMR ($CDCl_3$) δ 2.33 (s, 3H), 3.44 (s, 2H), 3.81 (s, 4H), 6.95–7.17 (m, 8H), 7.36–7.45 (m, 2H), 7.88–7.98 (m, 2H), 8.68–8.76 (m, 2H); ^{13}C NMR ($CDCl_3$) δ 20.9, 56.1, 58.0, 108.4, 120.6, 125.1, 127.3, 128.5, 129.4, 129.4, 134.1, 135.6, 136.5, 138.3, 147.2, 151.5; ESI-MS $m/z = 436$ ($[M + H]^+$, 100%). Compound **4b**: yield 16%; ^{1}H NMR (MeOD-d_4) δ 2.2 (s, 3H), 4.3 (s, 2H), 4.7 (s, 2H), 7.2–9.6 (m, 9H); ^{13}C NMR (MeOD-d_4) δ 21.8, 48.5, 48.8, 49.1, 49.8, 50.2, 50.5, 117.1, 124.7, 129.7, 131.4, 132.0, 137.0, 141.4, 145.5, 151.5; ESI-MS $m/z =$ 279 (free base, $[M + H]^+$, 100%).

*5.1.4. 5,5′-(4-(Trifluoromethyl)benzylazanediyl) bis(methylene)diquinolin-8-ol (JLK 1486, **5a**), 5-((4-(trifluoromethyl)benzylamino)methyl)quinolin-8-ol (**5b**) and tert-butyl (8-hydroxyquinolin-5-yl) methyl(4-(trifluoromethyl)benzyl)carbamate (**5c**)*

A solution of 5-chloromethylquinolin-8-ol dihydrochloride (300 mg, 1.3 mmol) and 4-(trifluoromethyl)benzylamine (683 mg, 3.9 mmol) in ethyl acetate (10 ml) is stirred at 50 °C overnight. It is cooled to 0 °C and filtered; the filter cake is washed with cold ethyl acetate (5 ml). The filtrate is concentrated in vacuo, diluted in diethyl ether (5 ml) and centrifuged. The ethereal phase is removed and the obtained solid is washed two more times by centrifugation with diethyl ether at 0 °C to give **5a** (32% yield); ^{1}H NMR ($CDCl_3$) δ 3.55 (s, 2H), 3.84

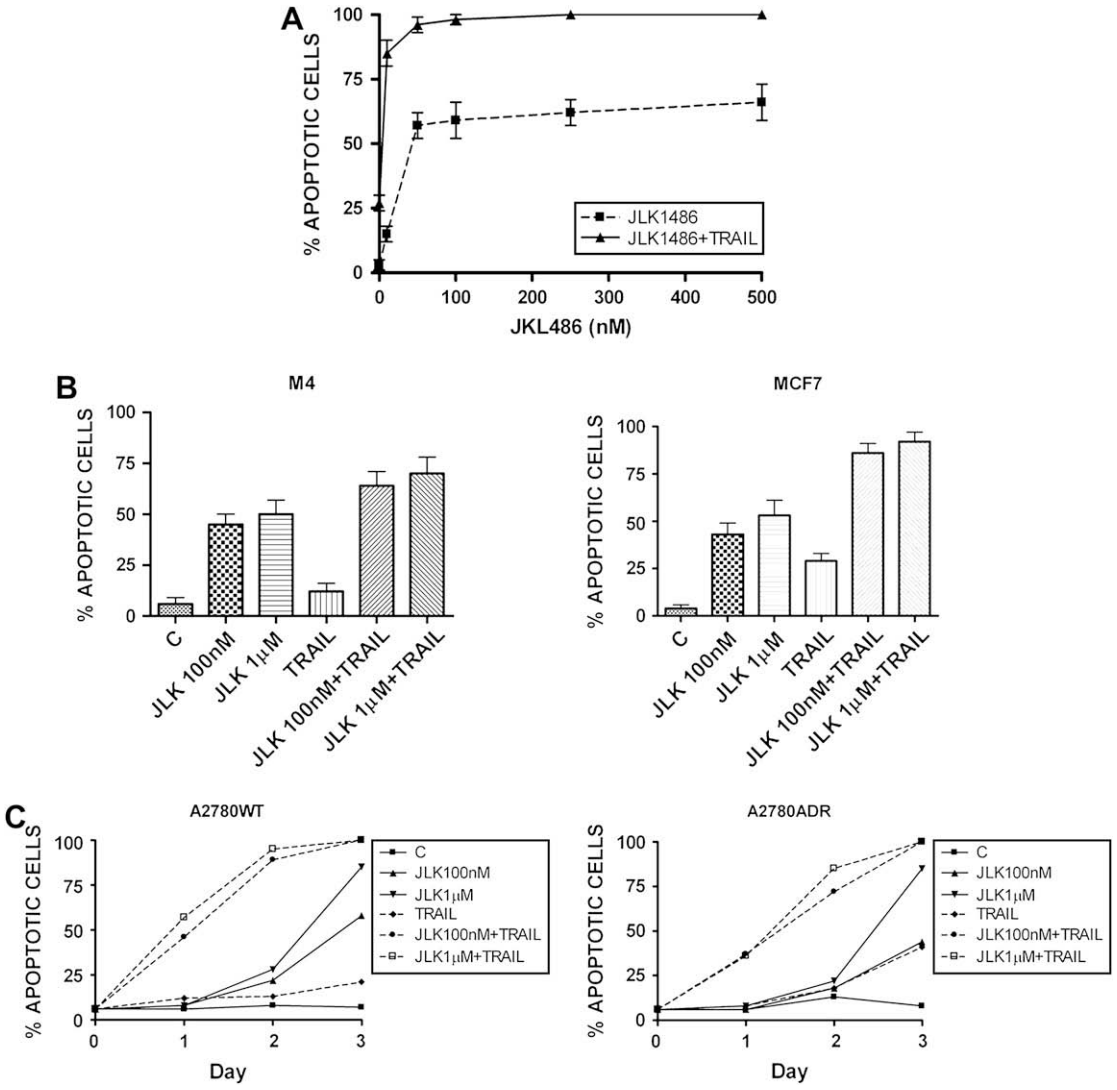

Fig. 7. *JLK 1486* markedly potentiates the cytotoxic effect of TRAIL on various cancer cell lines. (A) HL60 cell has been incubated for 24 h in the presence of increasing concentrations of *JLK 1486* added alone or in combination with recombinant human TRAIL (50 ng/ml), the percentage of apoptotic cells was determined by the Annexin V binding assay. Mean ± SEM are observed in three separate experiments. (B) Melanoma M4 and breast carcinoma MCF7 cells have been grown for 24 h either in the absence (C) or in the presence of *JLK 1486* (100 nM or 1 μM) added alone or in combination with TRAIL (50 ng/ml) or TRAIL at the above concentration and the proportion of apoptotic cells was evaluated as above. Mean values ± SEM are observed in three separate experiments. (C) Ovarian cancer A2780WT and its chemoresistant variant (A2780ADR) cell lines have been grown for various times (0–3 days) as reported in (B). The proportion of apoptotic cells was evaluated as above.

(s, 4H), 7.07–7.12 (m, 2H), 7.17 (m, 2H), 7.41 (m, 2H), 7.51 (m, 4H), 7.86 (m, 2H), 8.73 (m, 2H); ^{13}C NMR ($CDCl_3$) δ 30.9, 56.6, 58.1, 76.5, 77.0, 77.5, 108.7, 121.0, 124.7, 127.4, 129.8, 129.9, 133.9, 138.6, 147.6, 152.0; ESI-MS $m/z =$ 490 ($[M + H]^+$, 100%). Combined etheral phases are concentrated in vacuo. The obtained product is dissolved in dichloromethane (4 ml) and Boc_2O (171 mg, 0.786 mmol) is added. The solution is stirred overnight at room temperature then washed with water (4 ml) and brine (2 ml). It is dried over $MgSO_4$ then concentrated in vacuo and purified by chromatography eluting with cyclohexane–dichloromethane (1:1) to give **5b** (15% yield) as a white solid; ^{1}H NMR (DMSO-d_6) δ 4.40 (s, 2H), 4.67 (s, 2H), 7.44 (m, 1H), 7.82 (m, 3H), 7.95 (m, 2H), 9.07 (s, 1H), 9.24 (m, 1H), 9.93 (m, 1H); ESI-MS $m/z = 333$ ($[M + H]^+$, 100%). Compound **5c**: yield 19%; ^{1}H NMR (DMSO-d_6) δ 1.49 (s, 9H), 4.28 (s, 2H), 4.71 (s, 2H), 7.08 (m, 1H), 7.19 (m, 3H), 7.52 (m, 3H), 8.60 (m, 1H), 8.79 (m, 1H); ESI-MS $m/z = 433$ ($[M + H]^+$, 100%).

*5.1.5. 5,5′-(4-Nitrobenzylazanediyl) bis(methylene)diquinolin-8-ol (**6a**)*

A solution of 5-chloromethylquinolin-8-ol dihydrochloride (300 mg, 1.3 mmol), 4-nitrobenzylamine (123 mg, 0.65 mmol), and potassium carbonate (361 mg, 2.6 mmol) in dimethylformamide (20 ml) is stirred at 50 °C for 4 h. It is cooled to 0 °C and filtered; the filtered cake is washed with ethyl acetate (40 ml). The filtrate is washed with water (two times with 40 ml then six times with 20 ml), then the organic phase is dried over magnesium sulfate. It is then concentrated in vacuo, dissolved in diethyl ether (10 ml) and centrifuged. The

ethereal phase is removed and the obtained solid is washed two more times by centrifugation with diethyl ether at 0 °C to give 160 mg of **6a** (56% yield) as a green powder; ^{1}H NMR ($CDCl_3$) δ 3.5 (s, 2H), 3.9 (s, 4H), 7.1–8.8 (m, 14H); ^{13}C NMR ($CDCl_3$) δ 56.8, 57.9, 108.9, 121.1, 123.2, 124.4, 127.4, 130.0, 130.1, 133.6, 138.6, 147.0, 147.1, 147.6, 152.1; ESI-MS $m/z = 467$ ($[M + H]^+$, 100%).

5.1.6. 5,5′-(2-(Trifluoromethyl)benzylazanediyl) bis(methylene)diquinolin-8-ol (*7a*)

It was synthesized from 2-(trifluoromethyl)benzylamine following the procedure described for **3a** (33% yield); ^{1}H NMR ($CDCl_3$) δ 3.68 (s, 2H), 3.86 (s, 4H), 6.98 (m, 2H), 7.21–7.31 (m, 3H), 7.45 (m, 3H), 7.62 (m, 1H), 7.96 (m, 2H), 8.81 (m, 2H); ESI-MS $m/z = 490$ ($[M + H]^+$, 100%).

5.1.7. 5-((3-(Trifluoromethyl)benzylamino)methyl)quinolin-8-ol (*7b*) and 5-tert-butyl(8-hydroxyquinolin-5-yl)methyl (3-(trifluoromethyl)benzyl)carbamate (*7c*)

The compounds were synthesized from 3-(trifluoromethyl)-benzylamine following the procedure described for **5b** and **5c**. Compound **7b**: yield 15%; ^{1}H NMR (DMSO-d_6) δ 4.49 (s, 2H), 4.71 (s, 2H), 7.14 (m, 1H), 7.61–7.84 (m, 5H), 7.91 (m, 1H), 8.56 (m, 1H), 8.87 (m, 1H); ESI-MS $m/z = 333$ ($[M + H]^+$, 100%). Compound **7c**: yield 19%; ^{1}H NMR ($CDCl_3$) δ 1.49 (s, 9H), 4.28 (s, 2H), 4.82 (s, 2H), 7.07 (m, 1H), 7.21–7.26 (m, 2H), 7.30–7.37 (m, 3H), 7.42–7.49 (m, 3H), 8.78 (m, 1H); ESI-MS $m/z = 433$ ($[M + H]^+$, 100%).

5.1.8. (*S*)-5,5′-(1-Phenylethylazanediyl)bis(methylene) diquinolin-8-ol (*8a*), (*S*)-5-((1-phenylethylamino)methyl) quinolin-8-ol (*8b*), and (*S*)-tert-butyl(8-hydroxyquinolin-5-yl)methyl(1-phenylethyl)carbamate (*8c*)

The compounds were synthesized from (*S*)-1-phenylethanamine following the procedure described for **5a**, **5b** and **5c**. Compound **8a**: yield 32%; ^{1}H NMR ($CDCl_3$) δ 1.34 (d, 3H), 3.68–3.78 (m, 6H), 6.92 (m, 3H), 7.1–7.3 (m, 8H), 8.16 (m, 2H), 8.58 (m, 2H); ESI-MS $m/z = 436$ ($[M + H]^+$, 100%). Compound **8b**: yield 14%; ^{1}H NMR (MeOH-d_4) δ 1.79 (d, 3H), 4.47 (s, 2H), 4.73 (m, 2H), 7.45–7.65 (m, 6H), 7.91 (m, 1H), 8.14 (m, 1H), 9.0–9.15 (m, 2H); ^{13}C NMR (MeOH-d_4) δ 20.5, 47.3, 61.0, 116.7, 120.2, 124.5, 124.6, 129.5, 130.3, 131.0, 136.6, 137.4, 145.4, 145.6, 151.0; ESI-MS $m/z = 279$ (free base, $[M + H]^+$, 100%). Compound **8c**: yield 15%; ^{1}H NMR ($CDCl_3$) δ 1.27 (s, 9H), 1.45 (d, 3H), 4.55 (s, 2H), 4.82 (m, 2H), 7.1–7.4 (m, 6H), 8.15–8.45 (m, 2H), 8.65–8.75 (m, 2H); ESI-MS $m/z = 379$ ($[M + H]^+$, 100%).

5.1.9. 5,5′-(Naphthalen-1-ylmethylazanediyl)bis(methylene) diquinolin-8-ol (*9a*) and 5-((naphthalen-1-ylmethylamino) methyl)quinolin-8-ol dihydrochloride (*9b*)

The compounds were synthesized from 1-naphthylmethylamine following the procedure described for **3a** and **3b**. Compound **9a**: yield 4%; ^{1}H NMR ($CDCl_3$) δ 4.0–4.4 (m, 6H), 7.0–9.8 (m, 17H); ESI-MS $m/z = 472$ ($[M + H]^+$, 100%). Compound **9b**: yield 2%; ^{1}H NMR (MeOH) δ 4.5 (s, 2H), 4.8 (s, 2H), 7.4–8.2 (m, 12H); ESI-MS $m/z = 315$ (free base, $[M + H]^+$, 100%).

5.1.10. Ethyl quinoline-5-carboxylate (*11*)

It was synthesized from quinoline-5-carboxylic acid and the procedure has been described in Ref. [6]. Compound **11**: yield 70%; ^{1}H NMR ($CDCl_3$) δ 1.44 (t, 3H), 4.45 (q, 2H), 7.49 (m, 1H), 7.72 (m, 1H), 8.27 (m, 2H), 8.93 (m, 1H), 9.32 (m, 1H); ^{13}C NMR (MeOH-d_4) δ 14.3, 61.2, 122.4, 127.0, 127.1, 128.0, 130.6, 134.4, 134.7, 148.1, 150.5, 166.5; ESI-MS $m/z = 202$ ($[M + H]^+$, 100).

5.1.11. Quinolin-5-ylmethanol (*12*)

It was synthesized from ethyl quinoline-5-carboxylate and the procedure has been described in Ref. [6]. Compound **12**: yield 62%; ^{1}H NMR ($CDCl_3$) δ 5.13 (d, 2H), 7.43 (m, 1H), 7.55 (m, 1H), 7.65 (m, 1H), 8.03 (m, 1H), 8.50–8.53 (m, 1H), 8.87 (m, 1H); ^{13}C NMR (MeOH-d_4) δ 63.0, 121.1, 125.8, 126.5, 129.0, 129.7, 132.6, 136.8, 148.4, 150.1; ESI-MS $m/z = 160$ ($[M + H]^+$, 100).

5.1.12. 5-(Chloromethyl)quinoline (*13*)

A solution of quinolin-5-ylmethanol (160 mg, 1.0 mmol) in thionyl chloride (5 ml) is stirred 10 min at room temperature, then left 2 h at reflux. It is then concentrated in vacuo, dissolved in ethyl acetate and washed with brine. The organic phase is concentrated in vacuo to give 120 mg of crude **13** (67% yield) as a brown solid; ^{1}H NMR ($CDCl_3$) δ 5.00 (s, 2H), 7.46–7.67 (m, 3H), 8.10 (m, 1H), 8.48 (m, 1H), 8.95 (m, 1H); ^{13}C NMR (MeOH-d_4) δ 43.3, 121.4, 126.3, 128.0, 128.9, 130.9, 132.2, 133.4, 148.4, 150.3; ESI-MS $m/z = 178$ ($[M + H]^+$, 100).

5.1.13. 5,5′-(4-(Trifluoromethyl)benzylazanediyl) bis(methylene)diquinolin-8-ol (*14*)

It was synthesized from crude 5-(chloromethyl)quinoline and 4-(trifluoromethyl)benzylamine following the procedure described for **6a**. Compound **14**: yield 65%; ^{1}H NMR ($CDCl_3$) δ 5.23 (s, 2H), 5.56 (s, 4H), 7.28–7.39 (m, 3H), 7.51–7.85 (m, 5H), 8.41 (m, 2H), 8.72 (m, 2H), 8.95 (m, 4H); ESI-MS $m/z = 458$ ($[M + H]^+$, 100).

5.2. Biology

5.2.1. In vitro KB3-1 cell line assay

Human mouth epidermal carcinoma (KB) cell line was incubated for 72 h with different concentrations of drugs. The final volume in each experiment was made up with the media containing 1% DMSO final volume. Docetaxel was used as positive control. The experiments were performed in triplicate. Cell growth inhibition was determined by the MTS assay according to the recommendations of the manufacturer [Promega]. The optical density was measured at 490 nm. The number of viable cells was proportional to the extent of formazan production. The percent cytotoxicity index [(OD_{490} treated/OD_{490} control) × 100] was calculated from three experiments. For CC_{50} determinations, the cytotoxicity index was plotted against

the drug concentration ranged over 10–0.5 nM and the value resulting in 50% cytotoxicity was determined.

5.2.2. Tubulin and microtubule studies

Preparation of lamb brain tubulin. Tubulin was extracted from lamb brain by ammonium sulfate fractionation and ion-exchange chromatography and stored in liquid nitrogen. The protein was prepared as described [13–15]. Protein concentrations were determined spectrophotometrically with a Perkin–Elmer spectrophotometer Lambda 800 and an extinction coefficient at 275 nm of 1.09 L/g/cm in 6 M guanidine hydrochloride.

5.2.3. Tubulin assembly

Microtubule assembly was performed in 20 mM sodium phosphate buffer, 1 mM EGTA, 8 mM $MgCl_2$, 3.4 M glycerol, and 1 mM GTP pH 6.5. The reaction was started by warming the samples at 37 °C in thermostatted cuvettes (1 × 0.2 cm), and the mass of polymer formed was monitored by turbidimetry at 350 nm with a Beckman DU7400 spectrophotometer [15]. Samples containing the compound and their controls had less than 1% residual Me_2SO.

5.2.4. Proteasomal chymotrypsin-like assay

Whole cell extracts (10 μg) of cells treated with indicated compounds or mixtures were incubated for 2 h at 37 °C in 100 μl of assay buffer (50 mmol/L Tris–HCl, pH 7.5) with 10 μmol/L of fluorogenic substrate Suc-LLVY-AMC as described previously [16]. After incubation, production of free hydrolyzed 7-amino-4-methylcoumarin (AMC) groups liberated by substrate hydrolysis was fluorometrically measured using a Victor 3 Multilabel Counter with an excitation filter of 380 nm and an emission filter of 460 nm (Perkin–Elmer, Boston, MA, USA).

5.2.5. Caspase activity assay

Caspase activities were assayed in HL60 cell line after treatment with chemicals for 48 h. HL60 cells (20,000 cells per well in 180 μl RPMI medium) were plated in black 96-well culture microplates and treated with chemicals dissolved in DMSO (1% final volume). Plates were kept under 5% CO_2 for 48 h. Twenty microliters of 10× lysis buffer consisting in 250 mM Hepes (pH 7.5), 5 mM EDTA, 0.5% NP40, 0.1% SDS and 50 mM dithiothreitol was added before caspase substrates dissolved in water (DEVD-AMC and LEHD-AMC) or DMSO (IETD-AMC) at a final concentration of 50 μM. Plates were incubated at 37 °C and fluorescence was recorded ($\lambda_{exc} = 360$ nm, $\lambda_{em} = 435$ nm) at time 0, 30, 60, 120 and 180 min. Reaction rates were calculated from the slope of the linear time-dependent reaction and expressed as the fold-activation over the control (HL60 without chemical treatment). Colchicine 10^{-8} M was used as a positive control and processed as *JLK 1486* and *JLK 1472* added at concentrations 1, 0.1 and 0.01 μM.

5.2.6. Cytotoxic potentiation effect by TRAIL

The experimental procedure for these assays is described by Petrucci et al. [12].

Acknowledgments

The authors thank E. Coste and M. Toure for technical assistance and Prof. K. Dudley for critical reading of the manuscript. This work was supported by: Conseil Régional Provence Alpes Côte d'Azur, INSERM (Institut National de la santé et de la Recherche Médicale) (VM fellowship), CNRS (Centre National de la Recherche Scientifique), and IBDML (Institut de Biologie du Développement de Marseille-Luminy).

References

[1] S. Akiyama, A. Fojo, J.A. Hanover, I. Pastan, M.M. Gottesman, Isolation and genetic characterization of human KB cell lines resistant to multiple drugs, Somat. Cell Mol. Genet. 11 (1985) 117–126.
[2] A.Y. Chen, L.F. Liu, Design of topoisomerase inhibitors to overcome MDR1-mediated drug resistance, Adv. Pharmacol. 29B (1994) 245–256.
[3] A.K. Samraj, D. Sohn, K. Schulze-Osthoff, I. Schmitz, Loss of caspase-9 reveals its essential role for caspase-2 activation and mitochondrial membrane depolarization, Mol. Biol. Cell 18 (2007) 84–93.
[4] P.S. Schwartz, D.J. Waxman, Cyclophosphamide induces caspase 9-dependent apoptosis in 9L tumor cells, Mol. Pharmacol. 60 (2001) 1268–1279.
[5] J.H. Burckhalter, R.I. Leib, Amino- and chloromethylation of 8-quinolinol. Mechanism of preponderant *ortho* substitution in phenols under Mannich conditions, J. Org. Chem. 26 (1961) 4078–4083.
[6] C. Kaiser, P.A. Dandridge, E. Garvey, K.E. Flaim, R.L. Zeid, J.P. Hieble, Dopamine receptor agonist activity of some 5-(2-aminoethyl)carbostyril derivatives, J. Med. Chem. 28 (1985) 1803–1810.
[7] M.A. Jordan, L. Wilson, Microtubules and actin filaments: dynamic targets for cancer chemotherapy, Curr. Opin. Cell Biol. 10 (1998) 123–130.
[8] J.A. Evangelio, M. Abal, I. Barasoain, A.A. Souto, M.P. Lillo, A.U. Acuna, F. Amat-Guerri, J.M. Andreu, Fluorescent taxoids as probes of the microtubule cytoskeleton, Cell Motil. Cytoskeleton 39 (1998) 73–90.
[9] M. Di Vaira, C. Bazzicalupi, P. Orioli, L. Messori, B. Bruni, P. Zatta, Clioquinol, a drug for Alzheimer's disease specifically interfering with brain metal metabolism: structural characterization of its zinc(II) and copper(II) complexes, Inorg. Chem. 43 (2004) 3795–3797.
[10] D.A. Richards, Prophylactic value of clioquinol against travellers' diarrhoea, Lancet 1 (1971) 44–45.
[11] D. Chen, Q.C. Cui, H. Yang, R.A. Barrea, F.H. Sarkar, S. Sheng, B. Yan, G.P. Reddy, Q.P. Dou, Clioquinol, a therapeutic agent for Alzheimer's disease, has proteasome-inhibitory, androgen receptor-suppressing, apoptosis-inducing, and antitumor activities in human prostate cancer cells and xenografts, Cancer Res. 67 (2007) 1636–1644.
[12] E. Petrucci, L. Pasquini, A. Petronelli, E. Saulle, G. Mariani, R. Riccioni, M. Biffoni, G. Ferretti, P. Benedetti-Panici, F. Cognetti, G. Scambia, R. Humphreys, C. Peschle, U. Testa, A small molecule Smac mimic potentiates TRAIL-mediated cell death of ovarian cancer cells, Gynecol. Oncol. 105 (2007) 481–492.
[13] R.C. Weisenberg, G.G. Borisy, E.W. Taylor, The colchicine-binding protein of mammalian brain and its relation to microtubules, Biochemistry 7 (1968) 4466–4479.
[14] J.C. Lee, R.P. Frigon, S.N. Timasheff, The chemical characterization of calf brain microtubule protein subunits, J. Biol. Chem. 248 (1973) 7253–7262.
[15] J.M. Andreu, M.J. Gorbunoff, J.C. Lee, S.N. Timasheff, Interaction of tubulin with bifunctional colchicine analogues: an equilibrium study, Biochemistry 23 (1984) 1742–1752.
[16] C. Bailly, C. Bal, P. Barbier, S. Combes, J.P. Finet, M.P. Hildebrand, V. Peyrot, N. Wattez, Synthesis and biological evaluation of 4-arylcoumarin analogues of combretastatins, J. Med. Chem. 46 (2003) 5437–5444.